Deformable Image Registration and Intensity Correction of Cardiac Perfusion MRI

Mehran Ebrahimi(✉) and Sancgeetha Kulaseharan

Faculty of Science, University of Ontario Institute of Technology,
2000 Simcoe Street North, Oshawa, ON L1H 7K4, Canada
mehran.ebrahimi@uoit.ca, sancgeetha.kulaseharan@uoit.net

Abstract. Dynamic contrast Magnetic Resonance myocardial perfusion imaging has evolved into an accurate technique for the diagnosis of coronary artery disease. In this manuscript, we introduce and evaluate the performance of a non-rigid joint multi-level image registration and intensity correction algorithm on a common dataset. An objective functional is formed for which the corresponding Hessian and Jacobian is computed and employed in a multi-level Gauss-Newton minimization approach. In this paper, our experiments are based on elastic regularization on the transformation and total variation on the intensity correction. Our preliminary validations suggest that the registration scheme provides suitable motion correction if the parameters in the algorithm are properly tuned.

Keywords: Image registration · Inverse problems · Intensity correction · Optimization · Multi-level

1 Introduction

Dynamic contrast MR myocardial perfusion imaging has evolved into an accurate technique for the diagnosis of coronary artery disease. T1-weighted images are rapidly acquired every heartbeat to track the uptake and washout of a contrast agent. The diagnosis is based on time-series signal intensity data typically from rest and pharmacological stress images. Quantification of myocardial perfusion can be a useful adjunct to visual analysis, and can be valuable in other contexts. To quantify the time-series data, motion-free data is desired. However, at least 40 seconds of data are typically used to obtain regional perfusion values in the myocardium. Breath-holding becomes a major issue, particularly for patients and during pharmacological stress imaging. The problem is then to handle the inter-frame motion artefact caused by respiration, which makes quantitative analyses difficult.

In this manuscript, we present preliminary validations of a non-rigid joint motion and intensity correction algorithm that has been recently introduced in [4] and evaluate it on a common dataset. A key ingredient of the approach is the integration of intensity change compensation and motion correction into a unified

O. Camara et al. (Eds.): STACOM 2014, LNCS 8896, pp. 13–20, 2015.
DOI: 10.1007/978-3-319-14678-2_2

model. Rather than dividing the task into two sub-problems and treating these sub-problems sequentially and independently, the new approach assumes that these sub-problems are in fact related and mutually dependent. The algorithm is therefore based on a generalized variational framework, which integrates changes of positions and changes of intensities into a combined optimization framework. Recently in [5], a general PDE-framework for registration of contrast enhanced images was introduced. A PDE with a steady-state solution that corresponds to the solution of the described problem is derived and solved numerically. Furthermore, [14] model the intensity correction as a multiplicative term. However, this is not sufficient because loosely speaking if the intensity of a pixel is zero in one image and non-zero in another one, a multiplicative intensity correction factor cannot fix this. The scheme used in this manuscript is similar to [5], except that a more generalized regularization expression is employed. Furthermore, the more efficient Gauss-Newton approach in a multi-level implementation [13,15] is used as opposed to the steepest descent method in [5].

2 Data

The dataset consists of 10 cases from two centres: the University of Utah and University of Auckland. For each case, a single short axis slice time series at rest and at stress is provided. The Utah datasets were acquired using a saturation-recovery radial turboFLASH sequence at rest and during adenosine infusion ($140\ \mu g/kg/min$), as described in [3]. Contrast was 5 cc/s injection of Multihance (Gd-BOPTA) at 0.02 $mmol/kg$ for the rest and 0.03 $mmol/kg$ for the stress. Four of these subjects have known coronary artery disease. The Auckland cases were acquired using a saturation-recovery Cartesian turboFLASH sequence at rest and during adenosine infusion ($140\ \mu g/kg/min$). Contrast was 0.04 $mmol/kg$ Omniscan (gadodiamide). Expert-drawn contours were also provided at a chosen reference frame for each rest and stress case study.

3 Multi-level Joint Image Registration and Intensity Correction

Consider the registration problem of a template image $\mathcal{T}$ to a reference image $\mathcal{R}$, where $\mathcal{T}$ is a realization of $\mathcal{R}$ deformed via a transformation y and the intensity of this realization is changed via an extra additive [image] term w.

The d-dimensional reference and template images are represented by mappings $\mathcal{R}, \mathcal{T} : \Omega \subset \mathbb{R}^d \to \mathbb{R}$ of compact support. The goal is to find the transformation $y : \mathbb{R}^d \to \mathbb{R}^d$ and a compactly supported intensity correction image $w : \Omega \subset \mathbb{R}^d \to \mathbb{R}$ such that $\mathcal{T}[y] + w$ is similar to $\mathcal{R}$, in which $\mathcal{T}[y]$ is the transformed template image and $\mathcal{T}[y] + w$ is the intensity-corrected deformed image. A formulation of the joint image registration and intensity correction of a template image $\mathcal{T}$ to a reference image $\mathcal{R}$ can be written as the following problem.

Problem. Given two images $\mathcal{R}, \mathcal{T} : \Omega \subset \mathbb{R}^d \to \mathbb{R}$, find a transformation

$y : \mathbb{R}^d \to \mathbb{R}^d$ and an intensity correction image $w : \Omega \subset \mathbb{R}^d \to \mathbb{R}$ that minimize the joint objective functional

$$\mathcal{J}[y; w] := \mathcal{D}[\mathcal{T}[y] + w, \mathcal{R}] + \alpha\mathcal{S}[y - y^{\text{ref}}] + \beta\mathcal{Q}[w].$$

Here, $\mathcal{D}$ measures the dissimilarity of $\mathcal{T}[y] + w$ and $\mathcal{R}$, and $\alpha\mathcal{S} + \beta\mathcal{Q}$ is a regularization expression on $[y; w]$. It is assumed that $y^{\text{ref}}(x) = x$. Furthermore, sum of squared distances (SSD) is used as the dissimilarity measure, the elastic regularization is applied to the transformation [12,13], and the total variation (TV) [17,18] penalty is used on the additive intensity correction image. All of this can be summarized as

$$\begin{aligned}\mathcal{D}[\mathcal{T} + w, \mathcal{R}] &= \mathcal{D}^{\text{SSD}}[\mathcal{T} + w, \mathcal{R}] \\ &= \frac{1}{2}\int_\Omega (\mathcal{T}(x) + w(x) - \mathcal{R}(x))^2 \, dx,\end{aligned} \tag{1}$$

$$\mathcal{S}[y] = \frac{1}{2}\int_\Omega \mu\langle\nabla y, \nabla y\rangle + (\lambda + \mu)(\nabla \cdot y)^2 \, dx, \tag{2}$$

$$\begin{aligned}\mathcal{Q}[w] = \mathcal{TV}_\epsilon[w] &= \int_\Omega \sqrt{\|\nabla w(x)\|^2 + \epsilon} \, dx \\ &\approx \int_\Omega \|\nabla w(x)\| \, dx.\end{aligned} \tag{3}$$

Here we employ a discretize-then-optimize paradigm using a Gauss-Newton approach (see [13,15] and the FAIR software [13] for details) to minimize the functional in Equation (1). For practical implementations of the Hessian and Jacobian of the regularizer and the TV operators see [13,18]. We also consider different discrete representations of the joint image registration/intensity correction problem, and address the discrete problems sequentially in the so-called multi-level approach. Starting with the coarsest and thus inexpensive problem, a solution is computed, which then serves as a starting guess for the next finer discretization, see [13]. This procedure has several advantages. It adds additional regularization to the registration problem (more weight is given to more important structure), it is very efficient (typically, most of the work is done on the computationally inexpensive coarse representations, and only a refinement is required on the costly finest representation), it preserves the optimization character of the problem and thus allows the use of established schemes for line searches and stopping. The use of this technique leads to optimal schemes in the sense that only a fixed number of arithmetic operations is expected for every data point.

4 Results and Validation

We performed a series of pair-wise intensity-based registration experiments using the described method taking the reference image $R(\mathtt{x})$ as the frame for which the

expert-drawn contour is available. Here we present an example of these experiments for a pair of images in the stress case of 8-th dataset. The reference image in Figure 1(b) corresponds to the reference in stress case of study #8 (frame #21), and the template image Figure 1(a) is the last image in that sequence (frame #50). Using the multi-level Gauss-Newton approach, we are not only able to compute a reasonable displacement field Figure 1(d) but also an intensity correction term displayed in Figure 1(g). Due to this intensity correction term, we are now enabled to display the final registered and intensity corrected image $T(yc) + w(xc)$. In this experiment, we used the main parameters $\alpha = 50$, $\beta = 1$, $\epsilon = 1$, $\mu = 1$, and $\lambda = 0$, along with an Armijo line search [15] and a 2D linear interpolation [13]. The experimental result of our implementation is presented in Figure 1 for level 7, and the result of the previous levels 3 to 6 are displayed in Figure 2 (a) to (d). As it can be observed, the method has effectively separated the intensity changes of the two images being registered.

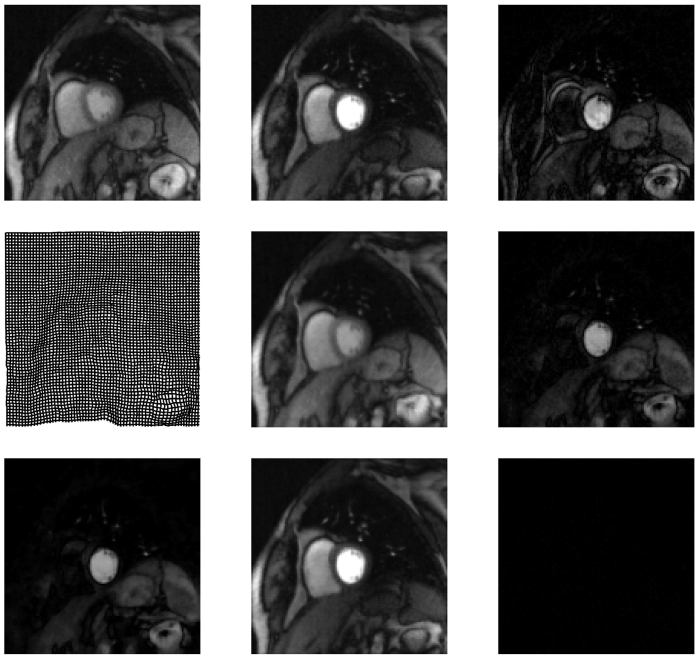

Fig. 1. Multi-level Gauss-Newton approach to joint image registration and intensity correction of stress dataset #8 for level 7:
(a) Template $T(\mathtt{x})$ (frame #50). (b) Reference $R(\mathtt{x})$ (frame #21). (c) $|T(\mathtt{x}) - R(\mathtt{x})|$.
(d) Grid $\mathtt{y}$. (e) Transformed template $T(\mathtt{y})$. (f) $|T(\mathtt{y}) - R(\mathtt{x})|$.
(g) Intensity correction $|\mathtt{w}(\mathtt{x})|$. (h) $T(\mathtt{y}) + \mathtt{w}(\mathtt{x})$. (i) $|T(\mathtt{y}) + \mathtt{w}(\mathtt{x}) - R(\mathtt{x})|$.

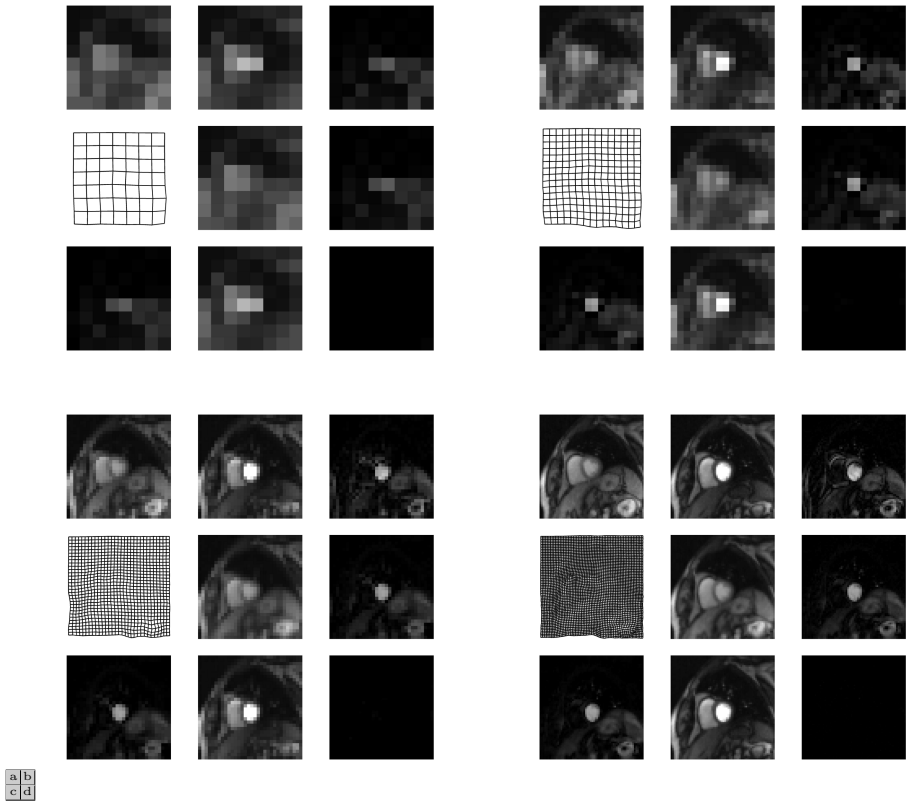

Fig. 2. Multi-level Gauss-Newton approach to joint image registration and intensity correction of stress dataset #8 for levels (a) 3. (b) 4. (c) 5. (d) 6. The order of displayed images are consistent with images displayed for the level 7 in Figure 1.

Figure 3 displays the final result for dataset #8, where the top row is relating to the rest and the bottom row is relating to to stress cases both taking frame #50 as the template and the corresponding references are frames #22 for rest and #21 for the stress case. The corresponding fixed location of contours for each case is also presented for comparison. It can be visually observed that the contours are correctly placed on the registered template images (c) and (f) compared to to their corresponding unregistered template images (b) and (e), while the motion is relatively smaller in the rest image (top row) compared to the stress image (bottom row).

Finally, Figure 4 shows results relating to dataset #8, top two rows are related to rest, and bottom 2 rows are related to stress. The graphs on the left and right respectively correspond to pre-registration and post-registration. Graphs on odd rows relate to tissue and AIF curves, and graphs on even rows represent Delta Si curves with model fits. Detailed information about obtaining these graphs is available in [16].

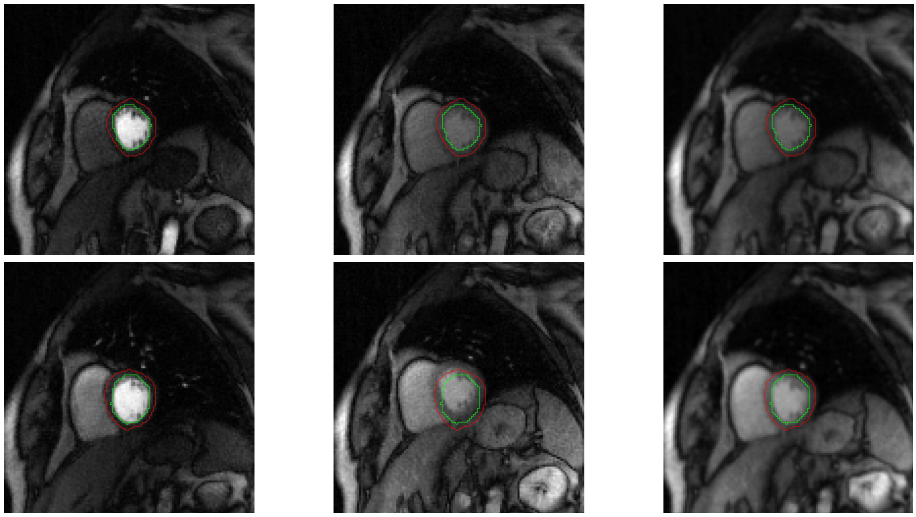

Fig. 3. Rest dataset #8:
(a) Reference (frame #22) (b) Template (frame #50) (c) Registered Template
Stress dataset #8:
(d) Reference (frame #21) (e) Template (frame #50) (f) Registered Template.

5 Discussion and Conclusion

It can be visually observed that the introduced algorithm has reasonably registered the pair of images. In addition, by comparing the tissue and AIF and Delta Si curves in Figure 4 before (left) and after (right) registration we realize smoother curves are obtained as a result of motion correction.

In our scheme, no prior rigid registration was performed on the acquired datasets. Choosing the main parameters of the algorithm, i.e. α and β, can significantly affect the result of the registration algorithm. These parameters are required to be tuned to yield superior registration results. A larger value of α allows less motion and attributes image intensity changes to the contrast enhancement. Inversely, a larger value of β tends to associate any variation of the image intensity to the motion, and allows the template image to move more freely which may lead to physically implausible motion in its extreme. In general, any registration algorithm requires setting a number of parameters and may fail if the parameters are not tuned properly. Finding a right balance among the parameters in our described algorithm proved to be challenging. Overall, the registration of the first five cases (1-5) was found to be more challenging than the last five cases (6-10) using our described method and we tried to further tune the parameters for the first five cases. As expected, registration of rest cases was found to be less challenging than the stress cases due to the fact that less motion was present in the rest image series.

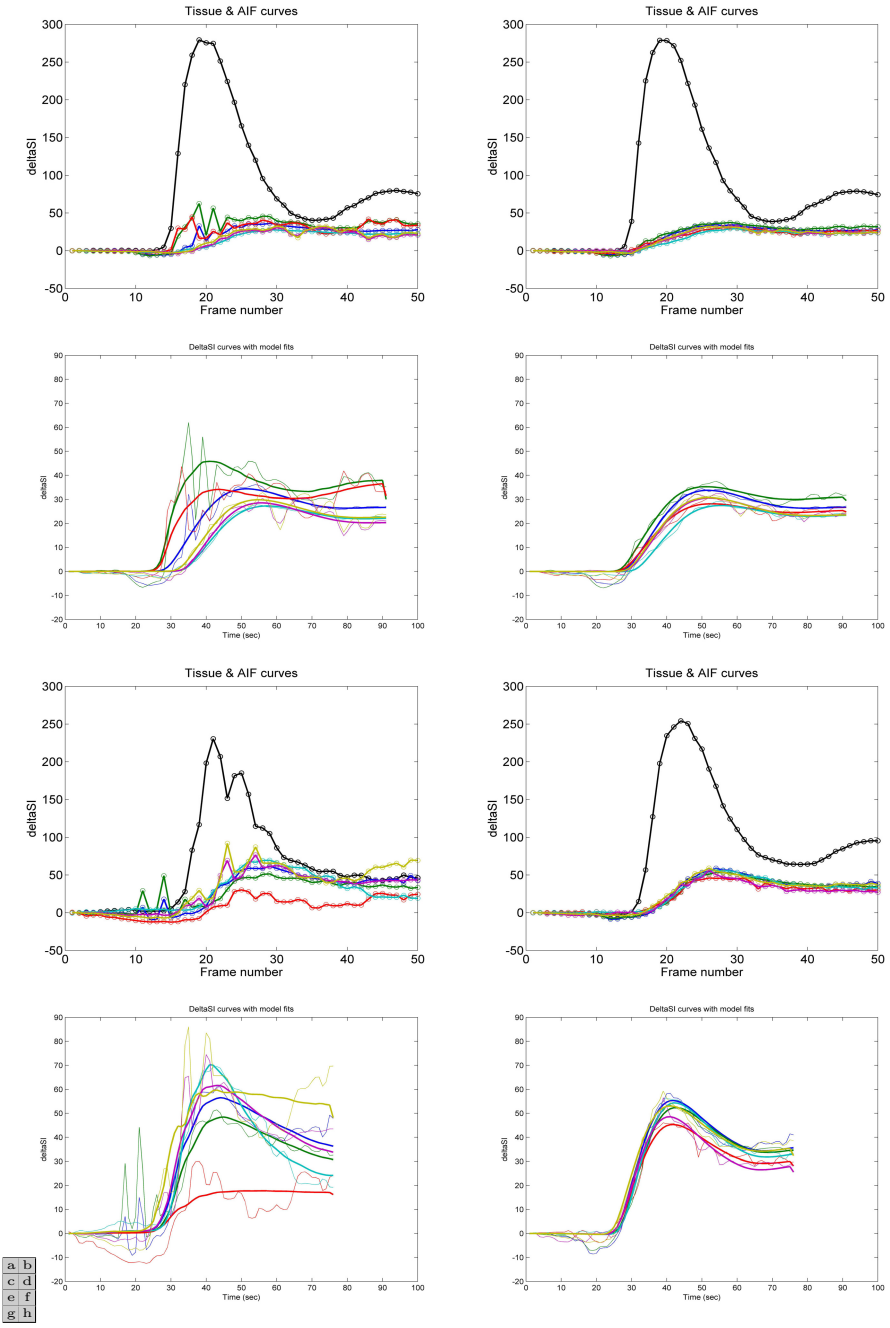

Fig. 4. Results relating to dataset #8, Top 2 rows: Rest, Bottom 2 rows: Stress, Left: Pre-registration, Right: Post-registration, Odd rows: Tissue and AIF curves, Even rows: Delta Si curves with model fits

Acknowledgments. This research was supported in part by the Natural Sciences and Engineering Research Council of Canada (NSERC) Discovery Grant of M. Ebrahimi. Undergraduate summer student research of S. Kulaseharan was supported by the University of Ontario Institute of Technology (UOIT).

References

1. Brown, L.G.: A survey of image registration techniques. ACM Computing Surveys **24**(4), 325–376 (1992)
2. Buonaccorsi, G.A., O'Connor, J.P.B., Caunce, A., Roberts, C., Cheung, S., Watson, Y., Davies, K., Hope, L., Jackson, A., Jayson, G.C., Parker, G.J.M.: Tracer kinetic model-driven registration for dynamic contrast-enhanced MRI time-series data. Magnetic Resonance in Medicine **58**(5), 1010–1019 (2007)
3. DiBella, E.V.R., et al.: The effect of obesity on regadenoson-induced myocardial hyperemia: a quantitative magnetic resonance imaging study. The International Journal of Cardiovascular Imaging **28**(6), 1435–1444 (2012)
4. Ebrahimi, M., Lausch, A., Martel, A.L.: A gauss-newton approach to joint image registration and intensity correction. Computer Methods and Programs in Biomedicine **112**(3), 398–406 (2013)
5. Ebrahimi, M., Martel, A.L.: A general pde-framework for registration of contrast enhanced images. In: Yang, G.-Z., Hawkes, D., Rueckert, D., Noble, A., Taylor, C. (eds.) MICCAI 2009, Part I. LNCS, vol. 5761, pp. 811–819. Springer, Heidelberg (2009)
6. Fischer, B., Modersitzki, J.: Ill-posed medicine - an introduction to image registration. Inverse Problems **24**, 1–19 (2008)
7. Ardeshir Goshtasby, A.: 2-D and 3-D Image Registration. Wiley Press, New York (2005)
8. Haber, E., Modersitzki, J.: A multilevel method for image registration. SIAM J. Sci. Comput. **27**(5), 1594–1607 (2006)
9. Hajnal, J., Hawkes, D., Hill, D.: Medical Image Registration. CRC Press (2001)
10. Hill, D.L.G., Batchelor, P.G., Holden, M., Hawkes, D.J.: Medical image registration. Physics in Medicine and Biology **46**, R1–R45 (2001)
11. Lausch, A., Ebrahimi, M., Martel, A.: Image registration for abdominal dynamic contrast-enhance magnetic resonance images. In: 8th IEEE International Symposium on Biomedical Imaging: From Nano to Macro, pp. 561–565 (2011)
12. Modersitzki, J.: Numerical methods for image registration. Oxford University Press, Oxford (2004)
13. Modersitzki, J.: (FAIR) Flexible Algorithms for Image Registration. SIAM (2009)
14. Modersitzki, J., Wirtz, S.: Combining homogenization and registration. In: Pluim, J.P.W., Likar, B., Gerritsen, F.A. (eds.) WBIR 2006. LNCS, vol. 4057, pp. 257–263. Springer, Heidelberg (2006)
15. Nocedal, J., Wright, S.J.: Numerical Optimization, 2nd edn. Springer (2006)
16. Pack, N., DiBella, E.V.R.: Comparison of myocardial perfusion estimates from dynamic contrast-enhanced magnetic resonance imaging with four quantitative analysis methods. Magnetic Resonance in Medicine **64**(1), 125–137 (2010)
17. Rudin, L.I., Osher, S., Fatemi, E.: Nonlinear total variation based noise removal algorithms. Physica D: Nonlinear Phenomena **60**(1–4), 259–268 (1992)
18. Vogel, C.R.: Computational Methods for Inverse Problems. SIAM (2002)

http://www.springer.com/978-3-319-14677-5

Statistical Atlases and Computational Models of the Heart: Imaging and Modelling Challenges
5th International Workshop, STACOM 2014, Held in Conjunction with MICCAI 2014, Boston, MA, USA, September 18, 2014, Revised Selected Papers
Camara, O.; Mansi, T.; Pop, M.; Rhode, K.; Sermesant, M.; Young, A. (Eds.)
2015, XII, 296 p. 134 illus., Softcover
ISBN: 978-3-319-14677-5